IMPROVED TREATMENT OF THE PHOTOIONIZATION PROCESS IN THE LASER INDUCED OPTICAL BREAKDOWN IN THE LASER TISSUE

Violeta PETROVIĆ[1] and Hristina DELIBAŠIĆ[1]

The development of laser technology led to the discovery that laser-living tissue (cells) interactions have significant biomedical applications and can be used to perform precise surgical procedures of 'water-like' tissues (such as the eye). When the focus is located within transparent biological cells and tissues, nonlinear absorption processes initiate a laser induced optical breakdown. The threshold for breakdown is defined by a certain critical free electron density. An in depth understanding of these processes orientated our theoretical research to the development of rate equations describing electron density growth in a transparent biological media exposed to a femtosecond laser pulse. In order to provide an accurate theoretical model and to predict damage occurrence, we took into account the losses through diffusion of electrons out of the focal volume, cascade ionization and the model of photoionization based on the standard Keldysh and ADK theory.

Keywords: laser-induced breakdown, avalanche process, Keldysh theory.

1. Introduction

The advent of high-power lasers opened the door for a wide range of laser application [1, 2, 3]. The effect known as the breakdown is a very important topic due to its role in laser applications. Breakdown is an effect which can be produced by high electric field strengths. This means that after a spark the medium becomes electrically conducting. Laser-induced breakdown (LIB) can occur in any media: solid, liquid, or gas. In this paper, we deal with laser-induced breakdown in water which is of great interest for laser applications in medicine. It has been shown experimentally that the optical breakdown in water is very similar to the liquid inside the eye and other biological media [4]. In laser eye surgery, the plasmas created by LIB in the eye are used to cut intraocular tissue [5].

High-power lasers are characterized with ultra-short pulses with extremely high intensities enabling deposition of laser energy into materials in a very efficient manner. The essence of a laser application is a physical picture known as a laser-matter interaction and ionization is the main process. For these intensities, the process is nonlinear [6]. Nonlinear processes became interesting with the

[1] Faculty of Science, University of Kragujevac, Kragujevac, Serbia, e-mail: hristinadelibasic@gmail.com

appearance of femtosecond lasers, which can be used to achieve very fine and highly localized laser effects inside biological media [6]. Before that, they were considered useless as their appearance was related to optical damage [7].

2. Theoretical background

The key point related to LIB is free electron density which can be produced through two steps. In the first, photoionization is the main process, while in the second, the obtained electrons produce electrons through effects known as secondary electron emission (SEE). The mechanisms behind SEE are based on the acceleration of free electrons through inverse Bremsstrahlung to high energies, which can lead to the avalanche process and breakdown of the material [8]. The critical electron density, as well as the critical field intensity of expected plasma creation, are also topics of interest.

The process of plasma formation through laser induced breakdown in the pure and transparent liquids (such as water) is schematically illustrated in Fig. 1 and it will be discussed in the text below.

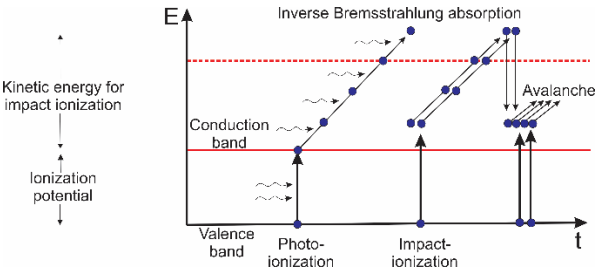

Fig. 1. Scheme of photoionization, inverse Bremsstrahlung and impact ionization in the process of LIB [9].

Comprehensive studies by Vogel and coworkers [6, 7, 9] have demonstrated that, generation of free electrons in the conduction band can be provided either by photoionization (tunneling or multiphoton ionization), or by impact ionization. Based on obtained results in [9], they concluded that when a free electron is produced in the medium it can absorb photons in a non-resonant process called inverse Bremsstrahlung absorption. After several successive events of inverse Bremsstrahlung absorption, the electron gains sufficiently large kinetic energy to produce additional electrons through impact ionization. This leads to an avalanche growth in the number of free electrons, while gained energy is required to overcome the energy loss by collisions with heavy particles occurring without simultaneous absorption of a photon. The whole process is called avalanche (or cascade) ionization. Because several consecutive inverse Bremsstrahlung absorption events are necessary for a free electron to pick up the critical energy for impact ionization,

there are time constraints for the avalanche ionization process. Recent experimental investigations yielded a value of the time before impact ionization can occur to be roughly 1 fs [9].

In this paper, we analyzed the probability for free electron creation in different processes which influence the whole process of laser-matter interaction, for femtosecond pulse duration. This is the main precondition for observing the free electron temporal density evolution. The atomic system of units $e = m_e = \hbar = 1$ is used throughout the paper [10].

According to [7, 9, 11] the time evolution of free electron density can be calculated using the complete rate equation which considers it as a cumulative contribution of the following relevant physical mechanisms:

$$\frac{d\rho_c}{dt} = w_{photo} + w_{casc}\rho_c + w_{term}\rho_c - w_{diff}\rho_c - w_{rec}{\rho_c}^2, \tag{1a}$$

$$\frac{d\rho_c}{dt} = \left(\frac{d\rho_c}{dt}\right)_{photo} + \left(\frac{d\rho_c}{dt}\right)_{casc} + \left(\frac{d\rho_c}{dt}\right)_{term} - \left(\frac{d\rho_c}{dt}\right)_{diff} - \left(\frac{d\rho_c}{dt}\right)_{rec}, \tag{1b}$$

where the first term represents the contribution of the photoionization, tunnel or multiphoton rate, $\left(\frac{d\rho_c}{dt}\right)_{photo}$, the second of the cascade (avalanche) effect, $\left(\frac{d\rho_c}{dt}\right)_{casc}$, and the third is the thermal ionization, $\left(\frac{d\rho_c}{dt}\right)_{term}$, while the last two terms describe the electron's losses through the processes of diffusion of free electrons from the focal volume and recombination respectively, $\left(\frac{d\rho_c}{dt}\right)_{diff}$ and $\left(\frac{d\rho_c}{dt}\right)_{rec}$. Diffusion is characteristic for nonlinear absorption and can significantly influence the observed process. From Eq. 1a, it can be seen that the cascade and diffusion rate are proportional to the first degree of the number of produced free electrons, while the recombination is proportional to the second because of possible electron and hole recombination. According to [7], the last two terms should not have a significant influence for the femtosecond, unlike nanosecond lasers. Our intention is, among other things, to check this claim by analyzing the contribution of all above-mentioned processes.

A Keldysh approach is usually used to describe the photoionization term. It has a wide range of applicability related to the value of the Keldysh parameter [12]. Keldysh introduced the well-known, Keldysh parameter, $\gamma = \omega\sqrt{2I_p}/F$, where ω is the laser frequency, I_p is the unperturbed ionization potential and F is the laser field strength used to distinguish two limiting regimes of the photoionization process. For $\gamma \gg 1$ (much higher than unity) multiphoton ionization is the dominant process, while for $\gamma \ll 1$ tunnel ionization is the dominant process. According to Keldysh [12], the photoionization term, $\left(\frac{d\rho_c}{dt}\right)_{photo}$, per electron, is given by the following expression:

$$\omega_K(\gamma, I_p, \omega) = \frac{2\omega}{9\pi}\left(\frac{\sqrt{1+\gamma^2}}{\gamma}\frac{\omega}{2}\right)^{\frac{3}{2}} Q\left(\gamma, \frac{I_p}{\omega}\right) \mathrm{Exp}\left\{-\pi\left\langle\frac{I_p}{\omega}+1\right\rangle \times,\right.$$
$$\left. \times \left[K\left(\frac{\gamma}{\sqrt{1+\gamma^2}}\right) - E\left(\frac{\gamma}{\sqrt{1+\gamma^2}}\right)\right] \Big/ E\left(\frac{\gamma}{\sqrt{1+\gamma^2}}\right)\right\}. \quad (2)$$

The bracket $\langle\ \rangle$ indicates the integer part of the photon's number necessary to ionize the target. The function $Q\left(\gamma, \frac{I_p}{\omega}\right)$ is defined through an elliptic integral of the first and second kind, $K(\mathrm{x})$ and $E(\mathrm{x})$, as well as the Dawson probability integral, $\Phi(\gamma, \mathrm{x})$ [12]:

$$Q(\gamma, \mathrm{x}) = \left[\pi/2K\left(\frac{1}{\sqrt{1+\gamma^2}}\right)\right]^{1/2} \times \sum_{n=0}^{\infty} \Phi\left\{\left[\pi^2(2\langle x+1\rangle - 2x + n)/2K\left(\frac{\gamma}{\sqrt{1+\gamma^2}}\right) \times\right.\right.$$
$$\left.\left. \times E\left(\frac{\gamma}{\sqrt{1+\gamma^2}}\right)\right]^{1/2}\right\} Exp\left[-\pi\left[K\left(\frac{\gamma}{\sqrt{1+\gamma^2}}\right) - E\left(\frac{\gamma}{\sqrt{1+\gamma^2}}\right)\right] n \Big/ E\left(\frac{\gamma}{\sqrt{1+\gamma^2}}\right)\right]. \quad (3)$$

To describe the corresponding density change, it is necessary to introduce the electron density in the ground state which corresponds to the total electron density at room temperature, $\rho_v = 6.68 \times 10^{22}\mathrm{cm}^{-3}$ [13] and free electron density, ρ_c. Now, the density change can be expressed as:

$$\left(\frac{d\rho_c}{dt}\right)_{\mathrm{photo}} = \omega_K(\gamma, I_p, \omega)(\rho_v - \rho_c). \quad (4)$$

But, how the femtosecond optical breakdown requires very high field intensities leading to very short tunneling time and $\gamma < 1$, it follows that tunnel ionization occupies an important place in the description of the femtosecond breakdown. Thus, we can introduce the most often used ADK theory to describe the photoionization rate [14]. In regard to [15], we tried to improve the commonly used Keldysh theory and, moreover, we compared these two approaches. Based on the ADK theory the photoionization rate can be calculated using the following formula [14]:

$$w_{ADK}(\gamma, F, \omega) = \left(\frac{4Z^3 e}{Fn^4}\right)^{2n-1} \mathrm{Exp}\left[-\frac{2Z^3}{3Fn^3} - \frac{p_0^2\gamma^3}{3\omega}\right], \quad (5)$$

where p_0 denotes the longitudinal component of the initial momentum, Z is the ion charge and n is the principal quantum number. Based on all aforementioned, we now suggest that a photoionization rate equation can be we rewritten as a sum of the rate for the tunnel and multiphoton regime as: $w_{photo} = w_{ADK} + w_{mp}$, where w_{mp} indicates the multiphoton limit of the general Keldysh equation [12] and w_{ADK} is the tunneling rate. Thus, the photoionization rate can be written as:

$$w_{photo}(\gamma, F, \omega, I_p) = \left(\frac{4Z^3 e}{Fn^4}\right)^{2n-1} \mathrm{Exp}\left[-\frac{2Z^3}{3Fn^3} - \frac{p_0^2\gamma^3}{3\omega}\right] + A\omega\left(\frac{I_p}{\omega}\right)^{3/2} \times$$

$$\times \mathrm{Exp}\left[2\left\langle\frac{I_p}{\omega}+1\right\rangle-\frac{2I_p}{\omega}\left(1+\frac{F^2}{2\omega^2 I_p}\right)\right]\times\left(\frac{F^2}{8\omega^2 I_p}\right)^{\frac{I_p}{\omega}+1}\Phi\left[\left(2\left\langle\frac{I_p}{\omega}+1\right\rangle-\frac{2I_p}{\omega}\right)^{1/2}\right]. \quad (6)$$

Ejected electrons obtained through the photoionization process, known as free electrons, can gain energy from the inverse Bremsstrahlung absorption [9] and induce impact ionization leading to an avalanche effect. The corresponding rate and electron density change are given respectively by [13]:

$$w_{casc}(\gamma,F,\omega,I_p)=\frac{1}{\omega^2\tau^2+1}\left[\frac{\tau}{cn_0(3/2)I_p}F-\frac{\gamma^2\tau}{M_m I_p}F^2\right], \quad (7a)$$

$$\left(\frac{d\rho_c}{dt}\right)_{\mathrm{casc}}=w_{casc}(\gamma,F,\omega)\times\rho_c, \quad (7b)$$

where τ is the time between collisions (according to [16] this time is approximately $\tau\sim$1fs for a femtosecond breakdown) and n_0 is the refractive index of the medium at a given frequency, ω and M_m is the mass of a water molecule. All values can be found in [16].

Researchers are strongly divided between two points of view. Some state that the femtosecond breakdown is mainly driven by multiphoton or tunneling ionization [17] and that the avalanche effect is minor, while others claim that the avalanche ionization dominates [18]. That is why we discussed the relative importance of photoionization and the avalanche effect in the sense of producing a breakdown. Also, an electron avalanche is considered to be a principal mechanism for laser pulses longer than a picosecond, but at the same time some measurements suggested that it is still significant in the femtosecond regime where it is expected that photoionization becomes the dominant process in free electron production [17].

To complete the picture of the LIB process, it is important to consider additional effects. First, we observed thermal ionization. The thermal ionization contribution (third term in Eq. 1b) is given by the formula [19]:

$$w_{therm}(\gamma,F,\omega,I_p)=\frac{\partial}{\partial t}T\left(\frac{3}{I_p}+\frac{1}{T}\right)\frac{3}{2}\sqrt{\frac{\pi}{2}}\left(\frac{T}{I_p}\right)^{1/2}\mathrm{Exp}\left(-\frac{I_p}{2T}\right), \quad (8a)$$

$$\left(\frac{d\rho_c}{dt}\right)_{\mathrm{therm}}=w_{therm}(\gamma,F,\omega,I_p)\times\rho_c, \quad (8b)$$

where T is the temperature in the focal volume of the laser [19]. The focal volume can be approximated in different ways. The most common are spherical and ellipsoidal [20]. In this case we assumed it to be ellipsoidal of a radius r_0 and length $z_R=\pi r_0^2/\lambda$ [13]. During the process of thermal ionization, the temperature rises in the focal volume, while the reproduced energy carried by the free electrons occurs within a few picoseconds to tens of picoseconds [9]. Findings of the performed experiment [21] undoubtedly indicated that for pulse durations longer than about 10 ps, large amounts of energy are reproduced from free electrons during the laser

pulse. This process results in a temperature increase to several thousand degrees Kelvin directly leading to a bright plasma luminescence.

Lastly, the last two terms in Eq. 1b represent processes that decrease the density of free electrons: diffusion and recombination. In LIB, one part of the electrons created in photo or cascade ionization can diffuse out of the focal volume. After diffusing, those electrons cannot play a role in furthering the avalanche process and, as a result, the density of the electrons will decrease. The appropriate rate formula for diffusion is given by expression [22]:

$$w_{diff}(I_p) = \frac{\tau I_p}{3}\left[\left(\frac{2.4}{r_0}\right)^2 + \left(\frac{1}{z_R}\right)^2\right], \tag{9a}$$

$$\left(\frac{\mathrm{d}\rho_c}{\mathrm{dt}}\right)_{diff} = w_{diff}(I_p) \times \rho_c. \tag{9b}$$

In the recombination event, free electrons become bound again by recombining with holes. With increasing free electron density recombination losses are larger because recombination is proportional to ${\rho_c}^2$. An empirical formula for density change can be used for the recombination term [23]:

$$\left(\frac{d\rho_c}{dt}\right)_{rec} = 2 \times 10^{-15}\ \mathrm{cm}^3/\mathrm{s} \times {\rho_c}^2 \tag{10}$$

In our results, we did not discuss recombination and thermal ionization. The reason for that is that we have empirical formulas for both of these processes and these terms do not qualitatively affect our results. These effects only influence the rate quantitatively while maintaining the rate's curve shape. Recombination was previously neglected also by [13,24]. Because of that, they were not of interest for us this time.

Following [25] it is assumed that water can be treated as an amorphous semiconductor with $I_p = 6.5$ eV. But, according to [22] this value should be changed to the autoionization threshold of $I_p = 9.5$ eV which can be understood in the sense of a band gap.

As mentioned in [15], the ionization potential has a significant role in ionization and LIB. In the following, we will discuss a corrected ionization potential.

For very short laser pulses, the ionization potential should be replaced by the effective ionization potential, ${I_p}^{eff}$, to account for the oscillation energy of the electron due to the electrical laser field, U_p, known as the ponderomotive potential. Additionally, we included splitting of energy levels through the linear Stark shift [26]:

$${I_p}^{eff} = I_p + U_p + E_{st} = I_p + \frac{F^2}{4\omega^2} + \frac{1}{2}\alpha F^2 = I_p\left(1 + \frac{1}{4\gamma^2}\right) + \frac{1}{2}\alpha F^2, \tag{11}$$

where α is the polarizability of a water molecule [27]. These inclusions lead to the effective ionization potential, ${I_p}^{eff}$, on which the rate depends exponentially.

3. Results and discussion

In this paper we focused primarily on the photoionization rate and compared the usually used Keldysh approach with ours, which considers a combination of the Keldysh and ADK approach. We observed the laser wavelength $\lambda = 800$ nm, with $100 -$ fs pulses and field intensities in the range $I = 10^{13} - 10^{15}$ Wcm^{-2}, focused into water. The mass of a water molecule is $M = 3 \times 10^{26}$ kg and the refractive index $n_0 = 1.33$. For these parameters, a free-electron density of $\rho_c \approx 2 \times 10^{19}$ cm^{-3} can be achieved [9]. We assumed that the unperturbated value of the ionization potential is $I_p = 0.21$ in atomic units [24]. The polarizability of a water molecule, α, is fixed to the value $\alpha \approx 9.6$ [27]. Because of the mentioned divided opinions about photoionization [17, 28], first, we were interested to discuss the role of tunneling and multiphoton ionization in the process of LIB, for different fixed values of field intensities.

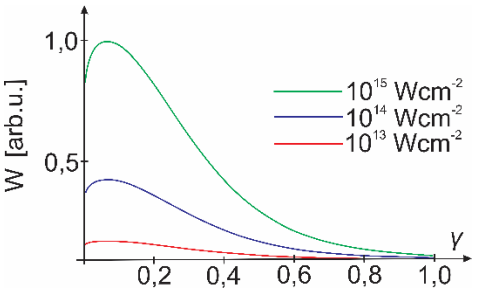

Fig. 2. Comparative review of the photoionization rate, $\omega_K(\gamma, I_p, \omega)$, for $\gamma = 0 - 1$, and for fixed laser field intensities, $I = 10^{13}, 10^{14}, 10^{15}$ Wcm^{-2}, red, blue and green line respectively.

In Fig. 2, we plotted the photoionization rate, based on Eq. 2, (Keldysh approach) for the Keldysh parameter in the range $\gamma = 0 - 1$ and for fixed laser intensities of $I = 10^{13}, 10^{14}, 10^{15}$ Wcm^{-2} respectively. The graphs clearly show that tunneling gives a large contribution to the photoionization rate for $\gamma < 0.4$ and that the photoionization contribution drastically decreases with γ approaching 1. It is obvious that this rate has a major contribution in the tunneling range while for the multiphoton one it is significantly lower. This is completely in accordance with [14]. Also, graphs show that the field increase leads to more significant domination of tunnel over multiphoton ionization.

Because of the dominant role of tunneling in the process of photoionization, we introduced the ADK theory to describe the photoionization rate in the tunnel domain, Eq. 5, while for multiphoton we used the Keldysh approach, Eq. 6, and as a result we obtained the comparative review shown in Fig. 3.

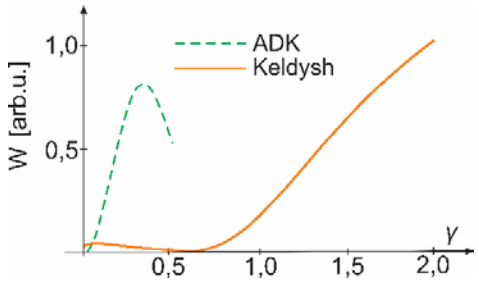

Fig. 3. Comparative review of photoionization rates, full Keldysh $\omega_K(\gamma, I_p, \omega)$ and cumulative, ADK and Keldysh, $w_{photo}(\gamma, F, \omega, I_p)$, for $\gamma = 0 - 2$, for a fixed laser field intensity, $I = 10^{14}$ Wcm^{-2}.

We fixed the field intensity to the value $I = 10^{14}$ Wcm^{-2} on which both ionization mechanisms can occur. The graph clearly shows that when γ is smaller than unity, $0 < \gamma < 0.5$, the tunneling rate predicted by the ADK theory is higher than the values predicted by Keldysh. In order to obtain results that are a closer representation of the real physical picture, we think that, for this range of values for which tunneling ionization is a dominant process, using ADK is a better approach. This behavior was completely expected and also experimentally confirmed numerous times [29, 30]. For γ larger than unity, multiphoton ionization becomes dominant and for this domain the Keldysh theory can be applied.

As we said our intention is to analyze photoionization, and in order to achieve it we observed the influence of additional processes on the ionization potential on which the rate exponentially depends. According to this, step by step, we included the ponderomotive potential and Stark shift, to obtain how the effective ionization potential affects the rate's curves. Incorporating the expression for effective ionization potential, Eq. 11, in Eq. 5 (for the ADK theory), and Eq. 6 (the Keldysh theory), we obtained curves presented in Fig. 4.

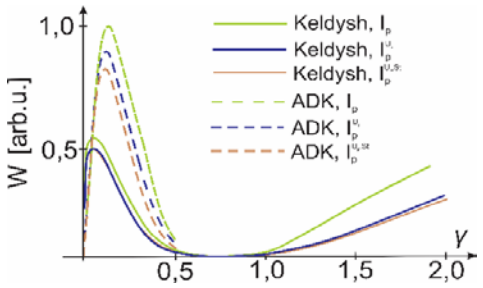

Fig. 4. Comparative review of photoionization rates, $\omega_K(\gamma, I_p, \omega)$ and $w_{photo}(\gamma, F, \omega, I_p)$, for $\gamma = 0 - 2$, for fixed laser field intensity, $I = 10^{14}$ Wcm^{-2}, without additional effects, with inclusion of ponderomotive potential and with inclusion of ponderomotive potential and Stark (green, blue and brown respectively).

From Fig. 4, it can be seen that the effective ionization potential influences the rate and that the ADK theory is significantly affected in the sense that inclusion of additional terms makes the rate lower and lower. For the same conditions, the Keldysh curve, in the tunneling range, is not sensitive to changes in the ionization potential. Inclusion of additional effects changes the multiphoton rate a little bit. Based on these results, which clearly show that the additional effect is important for understanding the whole physical background, we find that observing all effects is essential for improving the theoretical analysis of this physical process. Those effects are a magnetic field [31], excitation etc. that we are planning on reviewing in our future work.

Next, we observed the second phase of the free electron production and discussed the relative ratio between photo and cascade ionization. Based on Eq. 5, we obtained the cascade ionization rate curves for the intensities $I = 10^{13}, 10^{14}, 10^{15}$ Wcm^{-2} (Fig. 5a), and for fixed values of $\gamma = 0.1, 2, 4$ (Fig. 5b)

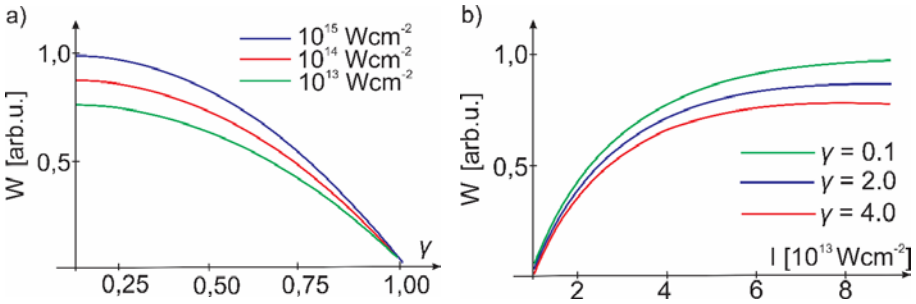

Fig. 5. Comparative review of cascade rates, $w_{casc}(\gamma, F, \omega, I_p)$a) for $\gamma = 0 - 1$ and fixed laser field intensities $I = 10^{13}, 10^{14}, 10^{15}$ Wcm^{-2}, b) for $\gamma = 0.1, 2, 4$ green, blue and red respectively and field intensity varying $I = 10^{13} - 9 \times 10^{13}$ Wcm^{-2}.

Related to the cascade rate, we observed that the field increase leads to a rate increase which was completely expected [9]. By fixing the Keldysh parameter to values that correspond to the tunneling and multiphoton range, we observed the highest rate to be for the value of the tunneling regime and declining for values that correspond to the multiphoton range. With higher values of the Keldysh parameter within the multiphoton range, the cascade rate is smaller which is in accordance with [7, 9].

We were interested to see which process is dominant, photo or cascade ionization within the observed conditions. To achieve this, we compared the obtained rates, $w_{photo}(\gamma, F, \omega, I_p)$ and $w_{casc}(\gamma, F, \omega, I_p)$, and the result is shown in Fig. 6.

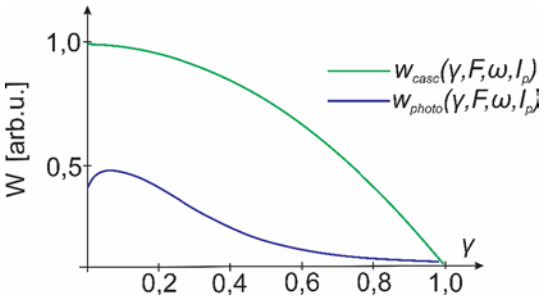

Fig. 6. Comparative review of photoionization, $w_{photo}(\gamma, F, \omega, I_p)$ and cascade rates, $w_{casc}(\gamma, F, \omega, I_p)$, for $\gamma = 0 - 1$, for a fixed laser field intensity. $I = 10^{14}$ Wcm^{-2}.

A significantly larger rate for cascade than photoionization for the entire range of values of γ is observed on Fig. 6. It is important to note that for higher values of laser field intensities there is a noticeable increase of the photoionization rate in the range of tunnel ionization. This behavior is in accordance with the previous conclusion that tunnel ionization becomes the dominant process over multiphoton and that creation of free electrons is concentrated in a narrow tunneling range. Based on the obtained curves, our results show that cascade ionization predominates over the photoionization process, in the whole range of the observed Keldysh parameter. That is why we can conclude that cascade ionization has the main role in the process of plasma creation [19, 28]

During the past decade, laser-tissue interaction in the femtosecond time regime has been extensively studied [32, 33]. In [34] it was clearly shown that when a fs laser pulse is incident onto a biological media, some of the abovementioned events occur. The timescale of the observed physical phenomena are represented in Table 1 [35, 36].

Table 1

Occurrence of the physical phenomena associated with laser–matter interaction

Physical phenomena involved in laser-material interaction	Time
photoionization (tunnelling or multiphoton ionization)	after 1 fs
cascade ionization	after 50 fs
thermalization of electrons	after 100 fs
thermal diffusion	after 1 ps
photochemical processes (chemical reactions or phase transitions)	after 1 ns

The nonlinear absorption of the fs–pulse energy is absorbed by the biological media and generates photoelectrons. First, after 1 fs, the pulse energy is transferred to electrons either by multiphoton absorption or tunnelling as long as the pulse is present. Cascade ionization dominates during the pulse time larger than 50 fs. About 50 fs afterwards, thermalization of electrons would take place. Longer laser pulse durations (greater than 1 ps) can influence the thermalization process and lead to thermal diffusion of electrons. This process defines the size of the

interaction region and it is directly related to the attenuation length of photons. Photochemical reactions occur for much longer laser pulses. After 1 ns, control of the pulse after pulse accumulated heat through the multiple-pulse irradiation is possible [34].

Finally, we incorporate the diffusion effect and as a result obtained the following graphs:

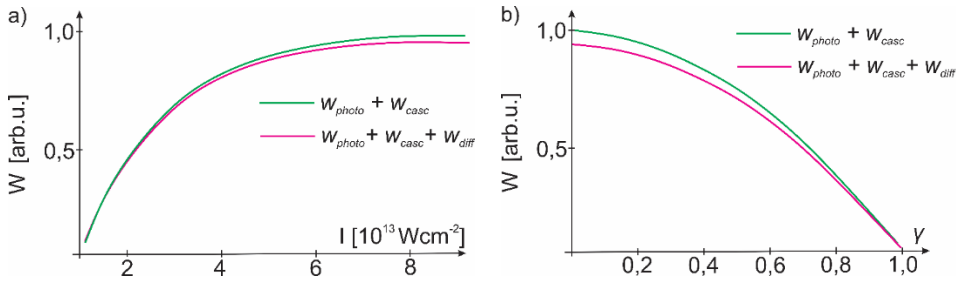

Fig. 7. Comparative review of contribution of the diffusion rate to the photo, $w_{photo}(\gamma, F, \omega, I_p)$, and cascade ionization, $w_{casc}(\gamma, F, \omega, I_p)$,: a) for fixed$\gamma = 0.01$, and laser field intensities, $I = 10^{13} - 10^{14}$ Wcm^{-2}, b) for fixed $I = 10^{13}$Wcm^{-2} and $\gamma = 0.001 - 1$.

In Fig.7, we wanted to analyze the effect of diffusion on the cumulative rate of photo and cascade ionization. It was previously considered that diffusion is not significant but we have observed a decrease in the rate over the entire range of laser field intensities, as well as the Keldysh parameter. According to [33], the diffusion loses are smaller for lower values of laser field intensities. The effect of diffusion becomes noticeable with increasing laser field intensities. Also, from Fig. 7b, we see that the influence of diffusion is larger in the range of tunneling ionization for approximately $\gamma < 0.5$ while for multiphoton ionization the influence decreases.

4. Conclusions

In this paper, we presented the results of an improved theory of breakdown in water. Based on the results shown in this paper, we can conclude that observing the photoionization rate as a cumulative contribution of ADK and Keldysh rates could potentially provide a better solution, in the frame of the striking agreement between theory and experiment, than the usually used Keldysh approach. We also found important inclusion of additional effects (ponderomotive potential and Stark shift). This approach could potentially provide a deeper understanding of the LIB process. Obtaining a more precise picture would allow for control of secondary electrons that are involved in the process of plasma creation.

Our results obtained in this paper can be used to update the basic assumptions for breakdown modeling in water which can be useful for the medical application of lasers.

Acknowledgement

This paper has been supported with the Serbian Ministry of Education, Science and Technological Development through Project 171020 and COST Action CA17126 “Towards understanding and modelling intense electronic excitation”.

R E F E R E N C E S

[1]. *A. Sussulini, J. S. Becker and J. S. Becker*, "Laser ablation ICP-MS: Application in biomedical research", in Mass spectrometry reviews, **vol. 36**, no. 1, 2017, pp. 47-57.

[2]. *M. Luo, F. Liang, Y. Song, D. Zhao, F. Xu, N. Ye and Z. Lin*, "M2B10O14F6 (M= Ca, Sr): two noncentrosymmetric alkaline earth fluosrooxoborates as promising next-generation deep-ultraviolet nonlinear optical materials", in Journal of the American Chemical Society, **vol. 140,** no. 11, 2018, pp. 3884-3887.

[3]. *A. Mena-Contla, V. N. Serkin, T. L. Belyaeva, R. Peña-Moreno, M. A. Agüero, C. Hernandez-Tenorio, and L. Morales-Lara*, “Extreme nonlinear waves in external gravitational-like potentials: possible applications for the optical soliton supercontinuum generation and the ocean coast line protection”, in Optik, **vol. 161**, 2018, pp. 187-195.

[4]. *F. Docchio*, “Lifetimes of plasmas induced in liquids and ocular media by single Nd: YAG laser pulses of different duration”, in Europhys Letters, **vol. 6**, no. 5, 1988, pp. 407-412.

[5]. *T. Sotiris, G. Nikolaos and G. Irini*, “Plexr: the revolution in blepharoplasty”, in Pinnacle Medicine & Medical Sciences, **vol. 1**, no. 5, 2014, pp. 423-427.

[6]. *A. Vogel, J. Noack, K. Nahen, D. Theisen, S. Busch, U. Parlitz, D. X. Hammer, G. D. Noojin, B. A. Rockwell and R. Bringruber*, “Energy balance of optical breakdown in water at nanosecond to femtosecond time scales”, in Applied Physics B, vol. 68, no. 2, 1999, pp. 271-280.

[7]. *A. Vogel, J. Noack, G. Hüttmanand and G. Paltauf*, “Mechanisms of femtosecond laser nanoprocessing of biological cells and tissues”, in Journal of Physics: Conference Series, **vol. 59**, no. 1, 2007, pp. 249.

[8]. *Yu. P. Raizer*, Gas discharge physics, Springer-Verlag, New York, 1991.

[9]. *A. Vogel, J. Noack, G. Huettmann and G. Paltauf*, “Mechanisms of femtosecond laser nanosurgery of cells and tissues”, in Applied Physics B, **vol. 81,** no. 8, 2005, pp. 1015-1047.

[10]. *R. McWeeny*, “Natural units in atomic and molecular physics”, in Nature, vol. 243, no. 5404, 1973, pp. 196-198.

[11]. *A. Bendib, K. Bendib-Kalache and C. Deutsch*, "Optical breakdown threshold in fused silica with femtosecond laser pulses", in Laser and Particle Beams, **vol. 31**, no. 3, 2013, pp. 523-529.

[12]. *L. V. Keldysh*, “Ionization in the field of a strong electromagnetic wave”, in Sov. Phys JETP, vol. 20, 1965, pp. 1307-1314.

[13]. *P. K. Kennedy*, “A first-order model for computation of laser-induced breakdown thresholds in ocular and aqueous media”, in IEEE Journal of Quantum Electronics, **vol. 31**, no. 12, 1995, pp. 2241-2249.

[14]. *M. V. Ammosov, N. B. Delone and V. P. Krainov*, “Multiphoton Processes in Atoms”, in Sov. Phys. JETP, **vol. 64**, 1986, pp.1191.

[15]. *V. E. Gruzdev*, “Laser-induced ionization of solids: back to Keldysh”, in Laser-Induced Damage in Optical Materials, **vol. 5647**, 2004, pp. 480-493

[16]. *M. Z. Ehteshami, M. R. Salehi and E. Abiri*, "Development of a numerical model to characterize laser-induced plasmas in aqueous media", in Journal of Optics, vol. 19, no. 9, 2017, pp. 095401.
[17]. *B. Rethfeld*, "Unified model for the free-electron avalanche in laser-irradiated dielectrics", in Physical review letters, **vol. 92**, no. 18, 2004, pp.187401.
[18]. *A. P. Joglekar, H. Liu, E. Meyhöfer, G. Mourou and A. J. Hunt*, "Optics at critical intensity: Applications to nanomorphing", in Proceedings of the National Academy of Sciences, **vol. 101**, no. 16, 2004, pp. 5856-5861.
[19]. *Y. R. Davletshin and J. C. Kumaradas*, "The role of morphology and coupling of gold nanoparticles in optical breakdown during picosecond pulse exposures", in Beilstein journal of nanotechnology, **vol. 7**, 2016, pp. 869.
[20]. *M. Lawrence-Snyder, J. Scaffidi, S. Michael Angel, A. P. M. Michael, and A. D. Chave*, "Sequential-pulse laser-induced breakdown spectroscopy of high-pressure bulk aqueous solutions" in Applied Spectroscopy, **vol. 61**, no.2, 2007, pp. 171-176.
[21]. *D. J. Stolarski, J. M. Hardman, C. M. Bramlette, G. D. Noojin, R. J. Thomas, B. A. Rockwell and W. P. Roach*, "Integrated light spectroscopy of laser-induced breakdown in aqueous media" in Laser-Tissue Interaction VI, **vol. 2391**, 1995, pp. 100-110.
[22]. *N. Linz, S. Freidank, X. X. Liang, H. Vogelmann, T. Trickl, and A. Vogel*, "Wavelength dependence of nanosecond infrared laser-induced breakdown in water: Evidence for multiphoton initiation via an intermediate state", in Physical Review B, vol. *91, no.* 13, 2015, pp.134114.
[23]. *P. K. Kennedy, D. X. Hammer and B. A. Rockwell*, "Laser-induced breakdown in aqueous media", in Progress in quantum electronics, **vol. 21**, no. 3, 1997, pp. 155-248.
[24]. *B. C. Stuart, M. D. Feit, S. Hermann, A. M. Rubenchick, B. W. Shore and M. D. Perry*, "Nanosecond-to-femtosecond laser-induced breakdown in dielectrics", in Physical review B, **vol. 53**, no. 4, 1996, pp. 1749-1761.
[25]. *J. Noack and A. Vogel*, "Laser-induced plasma formation in water at nanosecond to femtosecond time scales: calculation of thresholds, absorption coefficients, and energy density", in IEEE journal of quantum electronics, **vol.35**, no.8, 1999, pp. 1156-1167.
[26]. *K. L. Ishikawa*, "High-harmonic generation", in Advances in Solid State Lasers Development and Applications, 2010.
[27]. *G. Avila*, "Ab initio dipole polarizability surfaces of water molecule: Static and dynamic at 514.5 nm", in The Journal of Chemical Physics, **vol. 122**, no. 14, 2005, pp. 144310.
[28]. *D. Du, X. Liu and G. Mourou*, "Reduction of multi-photon ionization in dielectrics due to collisions", in Applied Physics B, **vol. 63**, no. 6, 1996, pp. 617-621.
[29]. *V. M. Gkortsas, S. Bhardwaj, C. J. Lai, K. H. Hong, E. L. Falcão-Filho, and F. X. Kärtner*, "Interplay of mulitphoton and tunneling ionization in short-wavelength-driven high-order harmonic generation", in Physical Review A, **vol. 84**, no. 1, 2011, p.013427.
[30]. *S. H. Lin, A. A. Villaeyes, Y. Fujimura*, Advances in Multi-photon processes and spectroscopy, World Scientific, **vol. 16**, 2004.
[31]. *H. Iftikhar , S. Bashir, A. Dawood , M. Akram, A. Hayat, K. Mahmood, A. Zaheer, S. Amin, and F. Murtaza*, "Magnetic field effect on laser-induced breakdown spectroscopy and surface modifications of germanium at various fluencies", in Laser and Particle Beams, **vol. 35**, no. 1, 2017, pp. 159-169.
[32]. *F. He, Y. Liao, J. Lin, J. Song, L. Qiao, Y. Cheng, and K. Sugioka*, "Femtosecond laser fabrication of monolithically integrated microfluidic sensors in glass", in Sensors, **vol. 14**, no. 10, 2014, pp.19402-19440.
[33]. *D. Tan, K. N. Sharafudeen, Y. Yue, and J. Qiu*, "Femtosecond laser induced phenomena in transparent solid materials: Fundamentals and applications", in Progress in Materials Science, **vol. 76**, 2016, pp.154-228.

[34]. *A. H. Hamad*, "Effects of different laser pulse regimes (nanosecond, picosecond and femtosecond) on the ablation of materials for production of nanoparticles in liquid solution", in High Energy and Short Pulse Lasers, IntechOpen, 2016.

[35]. *S. S. Mao, F. Quéré, S. Guizard, X. Mao, R. E. Russo, G. Petite and P.Martin*, "Dynamics of femtosecond laser interactions with dielectrics", in Applied Physics A, **vol. 79**, no. 7, 2004, pp.1695-1709.

[36]. *A. Royon, Y. Petit, G. Papon, M. Richardson and L. Canioni*, Femtosecond laser induced photochemistry in materials tailored with photosensitive agents, in Optical Materials Express, **vol. 1**, no. 5, 2011, pp.866-882.